Published in final edited form as:
J Neurosci. 2010 November 3; 30(44): 14695–14701. doi:10.1523/JNEUROSCI.1570-10.2010.

CAPACITANCE MEASUREMENTS OF REGULATED EXOCYTOSIS IN MOUSE TASTE CELLS

Aurelie Vandenbeuch[1,2], **Robert Zorec**[3], and **Sue C. Kinnamon**[1,2,*]

[1] Department of Otolaryngology, University of Colorado Denver, 12700 E. 19th Ave., Mail Stop 8606, Aurora, CO, USA

[2] Rocky Mountain Taste and Smell center, University of Colorado Denver, Aurora, CO, USA

[3] Laboratory of Neuroendocrinology-Molecular Cell Physiology, Institute of Pathophysiology, Faculty of Medicine, University of Ljubljana, Ljubljana, Slovenia, and Laboratory of Cell Engineering, Celica, BIOMEDICAL CENTER, Technology Park 24, 1000 Ljubljana, Slovenia

Abstract

Exocytosis, consisting of the merger of vesicle and plasma membrane, is a common mechanism used by different types of nucleated cells to release their vesicular contents. Taste cells possess vesicles containing various neurotransmitters to communicate with adjacent taste cells and afferent nerve fibers. However, whether these vesicles engage in exocytosis upon a stimulus is not known. Since vesicle membrane merger with the plasma membrane is reflected in plasma membrane area fluctuations, we measured membrane capacitance (C_m), a parameter linearly related to membrane surface area. To investigate whether taste cells undergo regulated exocytosis, we used the compensated tight-seal whole-cell recording technique to monitor depolarization-induced changes in C_m in the different types of taste cells. To identify taste cell types, mice expressing green fluorescent protein (GFP) from the TRPM5 promoter or from the GAD67 promoter were used to discriminate Type II and Type III taste cells, respectively. Moreover, the cell types were also identified by monitoring their voltage-current properties. The results demonstrate that only Type III taste cells show significant depolarization-induced increases in C_m, which were correlated to the voltage-activated calcium currents. The results suggest that Type III, but neither Type II nor Type I cells exhibit depolarization-induced regulated exocytosis to release transmitter and activate gustatory afferent nerve fibers.

Keywords

taste; neurotransmission; exocytosis; TRPM5; GAD67; patch clamp; membrane capacitance

INTRODUCTION

Taste buds are the transducing elements of gustatory sensation. Each taste bud houses between 50-100 taste cells, which extend from the basal lamina to the surface of the epithelium, where their apical processes protrude through a taste pore and encounter taste stimuli in the oral cavity. The basolateral regions of taste cells communicate sensory information to other taste cells and to gustatory nerve fibers, which course throughout the taste bud. Considerable progress has been made in identifying the taste receptor proteins and

* Corresponding author for taste cells: Department of Otolaryngology, University of Colorado Denver, Denver, CO, USA. sue.kinnamon@ucdenver.edu, for membrane capacitance measurements: Robert Zorec robert.zorec@mf.uni-lj.si.

downstream signaling effectors involved in taste transduction (Chandrashekar et al., 2006). However, much less is understood about how taste information is communicated from taste cells to afferent nerve fibers.

Taste buds comprise three types of cells, based on morphological, immunocytochemical, and functional criteria. Type I cells, called “glial-like” cells, express enzymes for inactivation and uptake of neurotransmitters (Lawton et al., 2000; Bartel et al., 2006) and are generally presumed to have a support function. Type I cells possess only voltage-gated outward currents (Medler et al., 2003; Romanov and Kolesnikov, 2006) and do not form synaptic contacts with afferent nerve fibers. Type II taste cells, also called “receptor” cells, possess the taste receptors and signaling effectors for bitter, sweet, and umami stimuli (Zhang et al., 2003; Clapp et al., 2004). These cells possess voltage-gated Na^+ and K^+ currents (Medler et al., 2003; Romanov and Kolesnikov, 2006) and generate action potentials to taste stimuli (Yoshida et al., 2006). Type II cells release ATP as a transmitter to activate purinergic receptors on afferent nerve fibers (Finger et al., 2005). These cells associate with nerve fibers, but lack voltage-gated Ca^{2+} channels and the typical presynaptic specializations (Clapp et al., 2006; DeFazio et al., 2006). ATP is released through gap junction hemichannels (Huang et al., 2007; Romanov et al., 2007; Dando and Roper, 2009). Recent data suggest, however, that Type II cells also express vesicular transporters for ATP (Iwatsuki et al., 2009), suggesting ATP may also be released by vesicular mechanisms. Type III taste cells, called “synaptic” cells, form conventional synapses with afferent nerve fibers (Yang et al., 2000; Yee et al., 2001). These cells are highly excitable with voltage-gated Na^+, K^+, and Ca^{2+} currents, and release serotonin and noradrenalin upon membrane depolarization (Huang et al., 2008) or ATP released from Type II taste cells (Huang et al., 2005; Huang et al., 2009). Type III taste cells express glutamic acid decarboxylase isoform GAD67, suggesting GABA also may be released as a neurotransmitter (DeFazio et al., 2006).

Fusion of vesicle membrane with the plasma membrane causes an increase in membrane surface area that can be measured with whole-cell patch-clamp as changes in membrane capacitance ($C_{m;}$ Neher and Marty, 1982). We report the first high-resolution C_m measurements of regulated exocytosis in taste cells. Using transgenic mice expressing GFP from cell type-specific promoters, we report that Type III taste cells exhibit depolarization-induced increases in C_m, which are correlated with voltage-activated calcium currents, suggesting that transmitter release from these cells is mediated by Ca^{2+}-dependent vesicular mechanisms.

MATERIALS AND METHODS

Mice and taste cell isolation

Breeding pairs of GAD67-GFP mice, obtained from Jackson Laboratories (Bar Harbor, ME, Stock 007677), were bred and used to identify Type III taste cells. Approximately 75% of Type III taste cells express GAD67 (DeFazio et al., 2006). TrpM5-GFP mice were bred and used to identify Type II taste cells, since TrpM5 is exclusively expressed in Type II taste cells (Clapp et al., 2006). These mice were a generous gift of Dr. Robert Margolskee (Mt. Sinai Med. School, New York, NY; now at Monell Chemical Senses Center, Philadelphia, PA). TrpM5 is the Ca^{2+}-activated monovalent-selective cation channel required for bitter, sweet and umami taste transduction (Perez et al., 2002; Zhang et al., 2003) and is a convenient marker for Type II taste cells. In this study we used only GAD67-GFP positive taste cells to identify Type III cells, since these cells represent only about 15% of the cells in the taste bud. For Type II cells, which make up approximately 35% of the taste bud, we used both TrpM5-GFP positive cells and unlabeled cells showing voltage-gated Na^+ and K^+

currents, but no voltage-gated Ca^{2+} current (Vandenbeuch and Kinnamon, 2009). Mice of both genders were used for these studies.

Circumvallate taste cells were isolated by a method adapted from Béhé et al. (Behe et al., 1990). Briefly, adult mice were sacrificed by CO_2 inhalation and cervical dislocation. The tongue was removed and about 0.2ml of an enzyme cocktail was injected between the epithelium and the underlying muscle. The enzyme cocktail consists of 1 mg/ml Collagenase B (Roche Indianapolis, IN), 3 mg/ml dispase II (Roche, Indianopolis, IN), and 1 mg/ml Trypsin inhibitor (Sigma St. Louis, MO) dissolved in 1 mg/ml Tyrode's. In some cases, 0.05 mg/ml elastase (Roche, Indianopolis, IN) was added to the enzyme cocktail to improve the ability to obtain seals with the membrane. The tongue was bubbled in oxygenated Ca^{2+}/Mg^{2+} -free Tyrode's containing BAPTA (2 mM; Invitrogen, Eugene, OR) for 45 min, or until the epithelium containing the taste buds could be gently separated from the underlying connective tissue. Individual taste cells and isolated taste buds were removed by gentle suction applied by mouth and plated onto polylysine-coated coverslips affixed to perfusion chambers (RF-20, Warner Instruments, Hamden, CT). In general, isolated taste cells remained viable for up to several hours after isolation. However, during recording, Ca^{2+} currents in some cells tended to run down quickly, allowing us to test only a few solutions on each cell. Taste cells were viewed with an Olympus IX71 inverted microscope equipped with DIC optics and epi fluorescence. All procedures were approved by the University of Colorado Denver Institutional Animal Care and Use Committee.

Solutions

The bath contained Tyrode's saline solution, consisting of 10 mM HEPES/NaOH (pH 7.4), 10 mM D-glucose, 1 mM Na-pyruvate, 140 mM NaCl, 4 mM $CaCl_2$, 1 mM $MgCl_2$, and 5 mM KCl. Barium Tyrode's (for isolation of Ca^{2+} currents) contained 136 mM TEA, 10 mM $BaCl_2$, 1 mM $MgCl_2$, 10 mM HEPES/NaOH (pH 7.4), 10 mM D-glucose, 1 mM Na-pyruvate, and 400 nM tetrodotoxin (TTX). In some experiments 0.5 mM $CdCl_2$ was added to Tyrode's to block voltage-gated Ca^{2+} currents (Medler et al., 2003). The intracellular pipette solution consisted of 140 mM KCl, 1 mM $CaCl_2$, 2 mM $MgCl_2$, 10 mM HEPES/KOH (pH 7.2), 11 mM EGTA, 2 mM ATP, and 0.4 mM GTP. In most experiments the pipette tip (only) was backfilled with KF solution (110 mM KF, 30 mM KCl, 1 mM $CaCl_2$, 2 mM $MgCl_2$, 10 mM HEPES/KOH (pH 7.2) and 11 mM EGTA), to assist in seal formation. The pre-filling of pipette solution by the KF solution did not affect either the voltage-dependence of the currents or the membrane capacitance change compared to a KCl solution. All salts were of highest grade available (Sigma Chemical Corporation, St. Louis, MO).

Electrophysiology and data analysis

Taste cells, whose input resistance typically exceeds 1 GΩ (Bigiani, 2001; Medler et al., 2003), were patch-clamped and their membrane capacitance (C_m) was measured by using the compensated tight-seal whole-cell recording technique (Neher and Marty, 1982; Marty and Neher, 1983; Zorec et al., 1991). Measurements were performed with a dual-phase lock-in patch-clamp amplifier with the 1 GΩ resistor in the head-stage (SWAM IIC, Celica, Ljubljana, Slovenia). A 1591 Hz sine wave (11.1 mV r.m.s.) was superimposed on a command potential (-70 mV) in whole cell recording. We coated fire-polished thick-wall pipettes (3 to 7 MΩ) with dental periphery wax and used a low level of bath solution (400 μl per coverslip) to reduce the slow drift of the real (*Re*) and imaginary (*Im*) part of the admittance signals. The imaginary signal is linearly related to changes in membrane capacitance, while the real part of the admittance signal is contributed mainly by membrane conductance and access conductance (Neher and Marty, 1982; Zorec et al., 1991). During the measurements, the phase setting of the lock-in amplifier was adjusted to nullify the

changes in the *Re* signal in response to a 100 fF calibration steps. For the frequencies of the sine-wave stimulation used (up to ~20 kHz), the phase determination by the capacitance dithering provides a suitable calibration value (Debus and Lindau, 2000). The criteria of correct phase setting were as described previously (Neher and Marty, 1982; Zorec et al., 1991; Henkel et al., 2000). Signals from the lock-in amplifier (*Re* and *Im* part of admittance signals were low pass filtered at 100 to 1kHz, -3 dB, 2-pole Bessel), together with the d.c. current (low pass filtered at 10 Hz, -3 dB,2-pole Bessel), unfiltered current and voltage were digitized at 10 kHz (DIGIDATA 1322A 16-bit data acquisition system and the CLAMPFIT 9.2 software suite, Molecular Devices, Sunnyvale, CA). Signals were additionally filtered by the filter options available with the CLAMPFIT 9.2 software.

When a fluorescent cell was identified under the microscope, we obtained a giga-seal whole-cell recording and read the resting membrane capacitance from the dials of the patchclamp amplifier. Following the phase adjustment (Fig. 1A), a series of 100 ms depolarizing voltage pulses in 10 mV increments was applied from the holding potential (-70 mV). This voltage series was repeated 10 times with a 100 ms interval and responses were averaged to reduce the noise level. For Fig. 5C, a single voltage series was used.

Secretory responses were measured by determining the change in amplitude of the *Im* signal, proportional to the membrane capacitance (C_m), recorded before and after each pulse. We measured the average amplitude value of a 50 ms signal epoch starting 60 ms prior to the voltage pulse and a 50 ms signal epoch starting 10 ms after the end of the voltage pulse (Fig. 1B, middle trace, bars). The change in average capacitance was measured for each cell and these measurements were averaged. These epochs were additionally filtered by a digital Gaussian filter (Clampfit facility, low pass, 100Hz). Close inspection of the middle trace of panel 1B shows that after the application of the voltage pulse, the amplitude of the averaged *Im* trace, representing changes in C_m, increased by approximately 3fF, without a correlated change in the *Re* part of the admittance signal, which reflects changes in membrane and access conductance. To insure that the voltage protocol application did not alter the phase setting, we repeated the phase adjustment following the voltage series (Fig. 1C). We also readjusted the phase following any solution changes to the recording chamber. All recordings were obtained at room temperature (~20° C).

All statistics are in the form of mean ± SEM unless otherwise stated. Statistical significance between averages was tested with a one-way ANOVAwith Tukey's Multiple Comparison Test (GraphPad Prism version 5).

RESULTS

Acutely isolated taste cells have an ovoid to elongated spindle or fusiform shape with a maximal diameter of 3 to 10 μm and a length of 15 to 30 μm (Fig. 2A, see also (Romanov et al., 2007), which appears slightly smaller in comparison to electron micrographs published previously (Kinnamon et al., 1988;Royer and Kinnamon, 1988). Membrane capacitance (C_m) is a parameter proportional to membrane surface area (Neher and Marty, 1982) and considering a specific membrane capacitance of 5 fF/μm^2 (equals 0.5 μF/cm^2) (Solsona et al., 1998) and assuming a cylindrical shape, an estimate of resting C_m from 1 to 8 pF is expected in taste cells. Measurements on 75 cells revealed a resting C_m of 3.42 ± 0.18 pF (mean ± SEM), consistent with values reported previously (Bigiani, 2001). Resting C_m of Type I cells, identified electrophysiologically (Figs. 2B-2D), (Medler et al., 2003;Romanov and Kolesnikov, 2006), was 4.25 ± 0.34 pF (n=19). Type III cells, identified by green fluorescence of GAD67-GFP mice (Fig. 2A, (DeFazio et al., 2006;Tomchik et al., 2007)) had a resting capacitance of 2. 60 ± 0.12 pF (n = 37), whereas Type II cells, identified by the green fluorescence of TRPM5-GFP mice and/or by the profile of voltage-activated inward

currents (Figs. 2B-2D), Medler et al., 2003;Clapp et al., 2006) exhibited a resting capacitance of 4.21 ± 0.46 pF (n = 19). Larger resting C_m of Type I and Type II taste cells ($P<0.001$) in comparison to Type III cells is consistent with their morphology (Royer and Kinnamon, 1994). Type I cells possess membranous extensions that envelop other taste cell types (Pumplin et al., 1997), contributing to their relatively high C_m for their apparent size.

To detect voltage-induced surface area changes monitored as C_m in the fF range and to monitor the voltage- activated currents, we applied a series of 9 depolarizing pulses (Fig. 3A) averaged over 10 cycles (to reduce noise) to determine whether the cell exhibited voltage-activated currents and showed concomitant changes in C_m. Fig. 3B shows representative responses to the averaged series of voltage pulses in the three types of taste cells. Note that at the highest voltage pulse amplitudes, significant increases in C_m are recorded in Type III cells (Figure 3B, top trace). In contrast, in Type II (Fig. 3B, middle trace) and in Type I (Fig 3B, bottom trace) cells such changes were not observed. Average changes in C_m (Fig 3C), measured before and after each voltage pulse, show that only in Type III cells voltage-induced increases in C_m are present. In the other two cell types, voltage-induced changes in C_m are not significantly different from zero. Moreover, when capacitance changes were normalized to the resting C_m of each cell and represented as a % of resting C_m, similar results were obtained (Table 1).

As shown in Fig. 2B, high voltage-activated Ca^{2+} currents, determined in the presence of extracellular Ba^{2+} (see methods), are expressed in Type III cells, consistent with previous reports (Medler et al., 2003;Romanov and Kolesnikov, 2006). A recent study demonstrated that the currents in the GAD67-GFP subset of Type III cells are carried primarily by P/Q type Ca^{2+} channels, since they are blocked by Ω-agatoxin IVA (Roberts et al., 2009). We confirmed that the peak Ba^{2+} currents in our preparation are blocked by Ω-agatoxin IVA, (data not shown). Since the general Ca^{2+} channel blocker Cd^{2+} is more readily reversible in our preparation, we elected to use Cd^{2+} to determine the Ca^{2+} dependence of the changes in C_m in Type III taste cells. Compared to the control (Fig. 4B), the application of 0.5 mM Cd^{2+} reduced the depolarization-induced C_m changes (Fig. 4C) and the effect was reversible (Fig. 4D). The effect was significant ($P<0.05$, n=5), based on the average of voltage-induced responses in C_m, determined from the last 5 voltage pulses in the series (Fig. 4E). Partial, rather than full, recovery is likely due to a time-dependent amplitude reduction of voltage-induced responses in C_m under control conditions, as shown on Fig 4F, where we observed a decline with a time-constant of around 8 minutes.

To further test the role of Ca^{2+}, we studied the relationship between voltage-induced increases in C_m and the amplitude of voltage-activated Ba^{2+} currents. Following the recording of voltage-induced changes in C_m in Type III cells (measured with Ca^{2+}-containing Tyrode's), we then recorded the voltage-activated Ba^{2+} currents (Fig. 2B, right panel) in the same cells. Fig. 5A shows the relationship between the average amplitude of voltage-activated Ba^{2+} currents as a function of membrane potential. The threshold of activation of these currents is related to the increase in voltage-induced changes in C_m, recorded in the same cells (Fig. 5B), however the C_m change did not decrease at voltages where the Ba^{2+} current begins to decrease. To determine if the lack of decrease in the C_m at higher voltage steps was due to averaging 10 runs, which might lead to Ca^{2+} buildup, we recorded C_m changes in taste cells with a single voltage series. Although the C_m changes in these cells were more variable due to the lack of averaging, they showed a clear decrease in C_m at higher voltage steps, paralleling the decrease in Ba^{2+} current at the same voltage steps. These results corroborate and extend the results obtained with Cd^{2+} and are consistent with the hypothesis that Type III taste cells exhibit Ca^{2+}-associated voltage-dependent changes in C_m, likely reflecting regulated exocytosis of transmitter.

DISCUSSION

The aim of this study was to test whether taste cells exhibit depolarization-induced regulated exocytosis, consistent with the fusion of vesicle membrane with the plasma membrane, as monitored by patch-clamp membrane capacitance measurements (Neher and Marty, 1982). We show that a sequence of depolarizing stimuli in Type III taste cells reliably evokes increases in C_m that are not observed in either Type II or Type I taste cells. Although the depolarization-evoked C_m responses in the taste cells are small compared to those of mammalian sensory receptors with ribbon synapses (i.e., 4-5 fF in taste cells compared to 30 to 40 fF for mouse vestibular hair cells; (Dulon et al., 2009) and > 100 fF for photoreceptors; (Innocenti and Heidelberger, 2008)), the responses are robust and repeatable. This finding is consistent with the comparatively small synaptic area in taste cells compared to hair cells and photoreceptors (Royer and Kinnamon, 1988; 1994). Further, capacitance changes in taste cells are likely to be Ca^{2+}-dependent, involving the entry of Ca^{2+} through the voltage-activated Ca^{2+} channels. C_m responses were inhibited by the Ca^{2+} channel blocker Cd^{2+} and the threshold voltage for C_m increases mirrored the threshold for voltage-dependent Ba^{2+} current activation. Further, when a single voltage series was used to stimulate the taste cells, there was a clear decline in C_m at higher voltages where the Ba^{2+} current is declining. It is interesting that there was no obvious linear relationship between Ca^{2+} current density and C_m change when 10 runs were averaged. Although membrane C_m peaked at the peak of the Ba^{2+} current, it did not decay with the decreasing Ba^{2+} current at high voltages. The lack of decrease of C_m at higher voltages may be due to a residual build up of intracellular Ca^{2+}, since the voltage pulses were separated by only 100 ms and the voltage series was averaged over 10 cycles. However, this rate of stimulation is physiological, since Type III cells are highly electrically excitable and generate trains of action potentials to taste stimuli (Yoshida et al., 2009). Repetitive voltage steps, such as paired pulse protocols are commonly used to test the presence of facilitation of current amplitudes. The augmentation of responses is thought to be due to a build-up of Ca^{2+}.

Type III taste cells contain two classes of vesicles: small clear synaptic vesicles with a diameter of 40 to 70 nm and vesicles with a dense core with a diameter of 90 to 120 nm (Royer and Kinnamon, 1994). Considering that Type III cells in mouse form on average 2 synapses with the afferent nerve, and that each presynaptic site consists of around 250 small clear vesicles, the fusion of all these vesicles with the plasma membrane upon stimulation will result in a surface area increase of the taste cell of around 4 μm^2, or an equivalent of 20 fF. Further, it was shown that there are approximately 5 dense-core vesicles per slice of 250 nm thickness in Type III taste cells (see Fig. 5 in Royer and Kinnamon, 1994). Considering that a synapse consists of 5 sections (Royer and Kinnamon, 1994), each synapse will contain approximately 25 dense-core vesicles. Assuming that all dense-core vesicles fuse with the plasma membrane upon stimulation, a membrane surface area of around 1 μm^2, or an equivalent of 5 fF is expected. These data, combined with our C_m measurements, suggest that approximately 20% of the vesicles are released in response to each depolarizing stimulus. Since this number is much lower than that observed with sensory cells with ribbon synapses that rely on fast communication with sensory afferents (Innocenti and Heidelberger, 2008; Dulon et al., 2009), it suggests that the readily releasable pool of vesicles in Type III taste cells is much lower. Alternatively, the relatively small increase in C_m may also be due to the ongoing endocytosis. A very small decline in C_m was observed during the first few voltage steps, which may reflect background endocytosis, especially since the data were averaged over a 10 pulse series (Fig. 3B, top trace and Fig. 4B, top and bottom traces). Moreover, at higher amplitude voltage steps, a more rapid decline in C_m was observed, which may reflect a more rapid component of endocytosis, observed in other sensory cells (Matthews, 1996). However, the observed slow decline of C_m was much slower that the voltage pulse duration, which should minimally affect the measured

increases in C_m. However, it can not be ruled out completely that the voltage-induced steps in C_m are somehow underestimated by the slow decline in C_m due to slow endocytosis.

An important question that remains is the identity of the transmitter(s) that are released by each type of vesicle. Both serotonin (Huang et al., 2005; Huang et al., 2009) and norepinephrine (Huang et al., 2008) are released from Type III taste cells, and both likely involve dense-core vesicles. The transmitter(s) contained in the small clear vesicles is not known, but could be GABA, since Type III cells express GAD67 (DeFazio et al., 2006). Further studies will be required to determine if Type III cells release GABA in response to depolarization.

The lack of depolarization-induced C_m changes in the other types of taste cells is noteworthy. Type I cells are similar to astrocytes (Lawton et al., 2000; Bartel et al., 2006) in expressing proteins for uptake and degredation of transmitters. Unlike astrocytes, Type I taste cells contain abundant, membrane-associated dense granules in the apical region supposedly released to contribute to the dense substance in the taste pore (Takeda and Hoshino, 1975). Recent data also suggest that Type I cells may play a role in transduction. They express the amiloride-sensitive Na^+ channel ENaC, suggesting that Type I cells may be the primary transducer of amiloride-sensitive salt taste (Vandenbeuch et al., 2008). How salt taste information is transmitted from Type I taste cells to the nervous system or neighboring cells is unclear. These cells do not form morphologically identifiable synapses with nerve fibers. Our data indicate that depolarization does not result in release of either vesicles or dense granules.

Type II cells release ATP via hemichannels composed of pannexin-1 and/or connexin subunits (Huang et al., 2007; Romanov et al., 2007; Dando and Roper, 2009) to activate P2X receptors on the afferent nerve fibers (Finger et al., 2005). However, Type II cells also contain some components of synaptic machinery, including synaptobrevin-2 (Yang et al., 2004) and synaptophysin (Asano-Miyoshi et al., 2009). In addition, Type II cells express several peptide transmitters, including glucagon-like peptide I (GLP-1) (Shin et al., 2008); neuropeptide Y (NPY), cholecystokinin (CCK), and vasoactive intestinal peptide (VIP) (Shen et al., 2005; Zhao et al., 2005; Herness and Zhao, 2009); and galanin (Seta et al., 2006). Further, many Type II cells express choline acetyltransferase and vesicular acetylcholine transporter (Ogura and Lin, 2005; Ogura et al., 2007) suggesting ACh may also be released. If and how these transmitter candidates are released remains in question. Romanov et al. (2007) demonstrated that ATP is released from Type II cells in response to depolarizing voltage steps, however our data appear to rule out voltage-regulated exocytosis. Type II cells utilize IP_3-mediated release of Ca^{2+} from intracellular stores in the transduction of bitter, sweet, and umami taste stimuli (Zhang et al., 2003), and this may provide sufficient intracellular Ca^{2+} to evoke vesicular exocytosis. Further experiments will be required to test this possibility.

Acknowledgments

We thank Dr. William Betz for the use of the SWAM IIC amplifier, Dr. Robert Margolskee for the TrpM5-GFP mice, and Ms. Catherine Anderson and Mr. Daniel Sanculi for technical assistance. We also thank Dr. Jack Kinnamon for helpful discussions and Drs. Thomas Finger and Katie Rennie for comments on the manuscript. This work was supported by the bilateral grant BI-US/08-10-034 awarded to RZ and SK; RZ is supported by grants # P3 310 0381, #J3 0133, #J3 0031, J3-9417 from the Research Agency of the Republic of Slovenia. SK is supported by NIH grants DC000766 and DC007495.

REFERENCES

Asano-Miyoshi M, Hamamichi R, Emori Y. Synaptophysin as a probable component of neurotransmission occurring in taste receptor cells. J Mol Histol. 2009; 40:59–70. [PubMed: 19253017]

Bartel DL, Sullivan SL, Lavoie EG, Sevigny J, Finger TE. Nucleoside triphosphate diphosphohydrolase-2 is the ecto-ATPase of type I cells in taste buds. J Comp Neurol. 2006; 497:1–12. [PubMed: 16680780]

Behe P, DeSimone JA, Avenet P, Lindemann B. Membrane currents in taste cells of the rat fungiform papilla. Evidence for two types of Ca currents and inhibition of K currents by saccharin. J Gen Physiol. 1990; 96:1061–1084. [PubMed: 2280253]

Bigiani A. Mouse taste cells with glialike membrane properties. J Neurophysiol. 2001; 85:1552–1560. [PubMed: 11287479]

Chandrashekar J, Hoon MA, Ryba NJ, Zuker CS. The receptors and cells for mammalian taste. Nature. 2006; 444:288–294. [PubMed: 17108952]

Clapp TR, Yang R, Stoick CL, Kinnamon SC, Kinnamon JC. Morphologic characterization of rat taste receptor cells that express components of the phospholipase C signaling pathway. J Comp Neurol. 2004; 468:311–321. [PubMed: 14681927]

Clapp TR, Medler KF, Damak S, Margolskee RF, Kinnamon SC. Mouse taste cells with G protein-coupled taste receptors lack voltage-gated calcium channels and SNAP-25. BMC Biol. 2006; 4:7. [PubMed: 16573824]

Dando R, Roper SD. Cell-to-cell communication in intact taste buds through ATP signalling from pannexin 1 gap junction hemichannels. J Physiol. 2009; 587:5899–5906. [PubMed: 19884319]

Debus K, Lindau M. Resolution of patch capacitance recordings and of fusion pore conductances in small vesicles. Biophys J. 2000; 78:2983–2997. [PubMed: 10827977]

DeFazio RA, Dvoryanchikov G, Maruyama Y, Kim JW, Pereira E, Roper SD, Chaudhari N. Separate populations of receptor cells and presynaptic cells in mouse taste buds. J Neurosci. 2006; 26:3971–3980. [PubMed: 16611813]

Dulon D, Safieddine S, Jones SM, Petit C. Otoferlin is critical for a highly sensitive and linear calcium-dependent exocytosis at vestibular hair cell ribbon synapses. J Neurosci. 2009; 29:10474–10487. [PubMed: 19710301]

Finger TE, Danilova V, Barrows J, Bartel DL, Vigers AJ, Stone L, Hellekant G, Kinnamon SC. ATP signaling is crucial for communication from taste buds to gustatory nerves. Science. 2005; 310:1495–1499. [PubMed: 16322458]

Henkel AW, Meiri H, Horstmann H, Lindau M, Almers W. Rhythmic opening and closing of vesicles during constitutive exo- and endocytosis in chromaffin cells. EMBO J. 2000; 19:84–93. [PubMed: 10619847]

Herness S, Zhao FL. The neuropeptides CCK and NPY and the changing view of cell-to-cell communication in the taste bud. Physiol Behav. 2009; 97:581–591. [PubMed: 19332083]

Huang YA, Maruyama Y, Roper SD. Norepinephrine is coreleased with serotonin in mouse taste buds. J Neurosci. 2008; 28:13088–13093. [PubMed: 19052199]

Huang YA, Dando R, Roper SD. Autocrine and paracrine roles for ATP and serotonin in mouse taste buds. J Neurosci. 2009; 29:13909–13918. [PubMed: 19890001]

Huang YJ, Maruyama Y, Dvoryanchikov G, Pereira E, Chaudhari N, Roper SD. The role of pannexin 1 hemichannels in ATP release and cell-cell communication in mouse taste buds. Proc Natl Acad Sci U S A. 2007

Huang YJ, Maruyama Y, Lu KS, Pereira E, Plonsky I, Baur JE, Wu D, Roper SD. Mouse taste buds use serotonin as a neurotransmitter. J Neurosci. 2005; 25:843–847. [PubMed: 15673664]

Innocenti B, Heidelberger R. Mechanisms contributing to tonic release at the cone photoreceptor ribbon synapse. J Neurophysiol. 2008; 99:25–36. [PubMed: 17989244]

Iwatsuki K, Ichikawa R, Hiasa M, Moriyama Y, Torii K, Uneyama H. Identification of the vesicular nucleotide transporter (VNUT) in taste cells. Biochem Biophys Res Commun. 2009; 388:1–5. [PubMed: 19619506]

Kinnamon JC, Sherman TA, Roper SD. Ultrastructure of mouse vallate taste buds: III. Patterns of synaptic connectivity. J Comp Neurol. 1988; 270:1–10. 56–17. [PubMed: 3372731]

Lawton DM, Furness DN, Lindemann B, Hackney CM. Localization of the glutamate-aspartate transporter, GLAST, in rat taste buds. Eur J Neurosci. 2000; 12:3163–3171. [PubMed: 10998100]

Marty, A.; Neher, E. Tight-seal whole-cell recording.. In: Sakmann, B.; Neher, E., editors. Single-Channel Recording. Plenum Publishing Corp.; New York: 1983. p. 107-113.

Matthews G. Synaptic exocytosis and endocytosis: capacitance measurements. Curr Opin Neurobiol. 1996; 6:358–364. [PubMed: 8794078]

Medler KF, Margolskee RF, Kinnamon SC. Electrophysiological characterization of voltage-gated currents in defined taste cell types of mice. J Neurosci. 2003; 23:2608–2617. [PubMed: 12684446]

Neher E, Marty A. Discrete changes of cell membrane capacitance observed under conditions of enhanced secretion in bovine adrenal chromaffin cells. Proc Natl Acad Sci U S A. 1982; 79:6712–6716. [PubMed: 6959149]

Ogura T, Lin W. Acetylcholine and acetylcholine receptors in taste receptor cells. Chem Senses. 2005; 30(Suppl 1):i41. [PubMed: 15738185]

Ogura T, Margolskee RF, Tallini YN, Shui B, Kotlikoff MI, Lin W. Immuno-localization of vesicular acetylcholine transporter in mouse taste cells and adjacent nerve fibers: indication of acetylcholine release. Cell Tissue Res. 2007; 330:17–28. [PubMed: 17704949]

Perez CA, Huang L, Rong M, Kozak JA, Preuss AK, Zhang H, Max M, Margolskee RF. A transient receptor potential channel expressed in taste receptor cells. Nat Neurosci. 2002; 5:1169–1176. [PubMed: 12368808]

Pumplin DW, Yu C, Smith DV. Light and dark cells of rat vallate taste buds are morphologically distinct cell types. J Comp Neurol. 1997; 378:389–410. [PubMed: 9034899]

Roberts CD, Dvoryanchikov G, Roper SD, Chaudhari N. Interaction between the second messengers cAMP and Ca2+ in mouse presynaptic taste cells. J Physiol. 2009; 587:1657–1668. [PubMed: 19221121]

Romanov RA, Kolesnikov SS. Electrophysiologically identified subpopulations of taste bud cells. Neurosci Lett. 2006; 395:249–254. [PubMed: 16309836]

Romanov RA, Rogachevskaja OA, Bystrova MF, Jiang P, Margolskee RF, Kolesnikov SS. Afferent neurotransmission mediated by hemichannels in mammalian taste cells. Embo J. 2007; 26:657–667. [PubMed: 17235286]

Royer SM, Kinnamon JC. Ultrastructure of mouse foliate taste buds: synaptic and nonsynaptic interactions between taste cells and nerve fibers. J Comp Neurol. 1988; 270:11–24. 58–19. [PubMed: 3372732]

Royer SM, Kinnamon JC. Application of serial sectioning and three-dimensional reconstruction to the study of taste bud ultrastructure and organization. Microsc Res Tech. 1994; 29:381–407. [PubMed: 7858318]

Seta Y, Kataoka S, Toyono T, Toyoshima K. Expression of galanin and the galanin receptor in rat taste buds. Arch Histol Cytol. 2006; 69:273–280. [PubMed: 17287581]

Shen T, Kaya N, Zhao FL, Lu SG, Cao Y, Herness S. Co-expression patterns of the neuropeptides vasoactive intestinal peptide and cholecystokinin with the transduction molecules alpha-gustducin and T1R2 in rat taste receptor cells. Neuroscience. 2005; 130:229–238. [PubMed: 15561439]

Shin YK, Martin B, Golden E, Dotson CD, Maudsley S, Kim W, Jang HJ, Mattson MP, Drucker DJ, Egan JM, Munger SD. Modulation of taste sensitivity by GLP-1 signaling. J Neurochem. 2008; 106:455–463. [PubMed: 18397368]

Solsona C, Innocenti B, Fernandez JM. Regulation of exocytotic fusion by cell inflation. Biophys J. 1998; 74:1061–1073. [PubMed: 9533718]

Takeda M, Hoshino T. Fine structure of taste buds in the rat. Arch Histol Jpn. 1975; 37:395–413. [PubMed: 143255]

Tomchik SM, Berg S, Kim JW, Chaudhari N, Roper SD. Breadth of tuning and taste coding in mammalian taste buds. J Neurosci. 2007; 27:10840–10848. [PubMed: 17913917]

Vandenbeuch A, Clapp TR, Kinnamon SC. Amiloride-sensitive channels in type I fungiform taste cells in mouse. BMC Neurosci. 2008; 9:1. [PubMed: 18171468]

Yang R, Stoick CL, Kinnamon JC. Synaptobrevin-2-like immunoreactivity is associated with vesicles at synapses in rat circumvallate taste buds. J Comp Neurol. 2004; 471:59–71. [PubMed: 14983476]

Yang R, Crowley HH, Rock ME, Kinnamon JC. Taste cells with synapses in rat circumvallate papillae display SNAP-25-like immunoreactivity. J Comp Neurol. 2000; 424:205–215. [PubMed: 10906698]

Yee CL, Yang R, Bottger B, Finger TE, Kinnamon JC. "Type III" cells of rat taste buds: immunohistochemical and ultrastructural studies of neuron-specific enolase, protein gene product 9.5, and serotonin. J Comp Neurol. 2001; 440:97–108. [PubMed: 11745610]

Yoshida R, Shigemura N, Sanematsu K, Yasumatsu K, Ishizuka S, Ninomiya Y. Taste responsiveness of fungiform taste cells with action potentials. J Neurophysiol. 2006; 96:3088–3095. [PubMed: 16971686]

Yoshida R, Miyauchi A, Yasuo T, Jyotaki M, Murata Y, Yasumatsu K, Shigemura N, Yanagawa Y, Obata K, Ueno H, Margolskee RF, Ninomiya Y. Discrimination of taste qualities among mouse fungiform taste bud cells. J Physiol. 2009; 587:4425–4439. [PubMed: 19622604]

Zhang Y, Hoon MA, Chandrashekar J, Mueller KL, Cook B, Wu D, Zuker CS, Ryba NJ. Coding of sweet, bitter, and umami tastes: different receptor cells sharing similar signaling pathways. Cell. 2003; 112:293–301. [PubMed: 12581520]

Zhao FL, Shen T, Kaya N, Lu SG, Cao Y, Herness S. Expression, physiological action, and coexpression patterns of neuropeptide Y in rat taste-bud cells. Proc Natl Acad Sci U S A. 2005; 102:11100–11105. [PubMed: 16040808]

Zorec R, Henigman F, Mason WT, Kordas M. Electrophysiological study of hormone secretion by single adenohypophyseal cells. Methods in Neurosciences. 1991; 4:194–210.

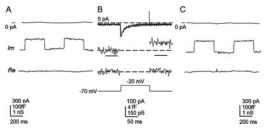

Figure 1. Protocol for capacitance measurements

(A) Membrane capacitance (C_m) measurements were performed by initially monitoring membrane current (top trace), filtered at 10Hz (low pass, -3dB, Bessel), at a holding potential -70 mV, to which a sine wave of 1591 Hz (11.1. mV r.m.s) was summed. Simultaneously we monitored imaginary (*Im*) and real (*Re*) part of admittance signals (200Hz low pass, Gaussian filter), which were used to set the phase by the calibrated 100fF capacitance step. (B) The recording of the voltage-induced current (3kHz, low pass, -3dB, 2-pole, Bessel) stimulated by a voltage step from -70 mV to -20 mV in a Type III taste cell. Note that after the pulse application there was a small increase in the *Im* part of the signal (low pass, 200 Hz, Gaussian filter), reporting a 3.26 ± 1.7 fF increase in C_m, there was however no change in the *Re* part of the signal (200 Hz, low pass, Gaussian filter). The voltage-induced change in C_m was significantly different from the C_m value prior to the pulse ($P<0.001$, Student's T-test). Horizontal bars beneath the middle *Im* trace show epochs of 50 ms, during which the amplitude of the change in C_m was determined. (C) To test whether the application of a series of voltage pulses induced a phase shift in the measuring system, we routinely monitored the phase angle setting at the end of the recording, where signals are shown at the same settings as in (A).

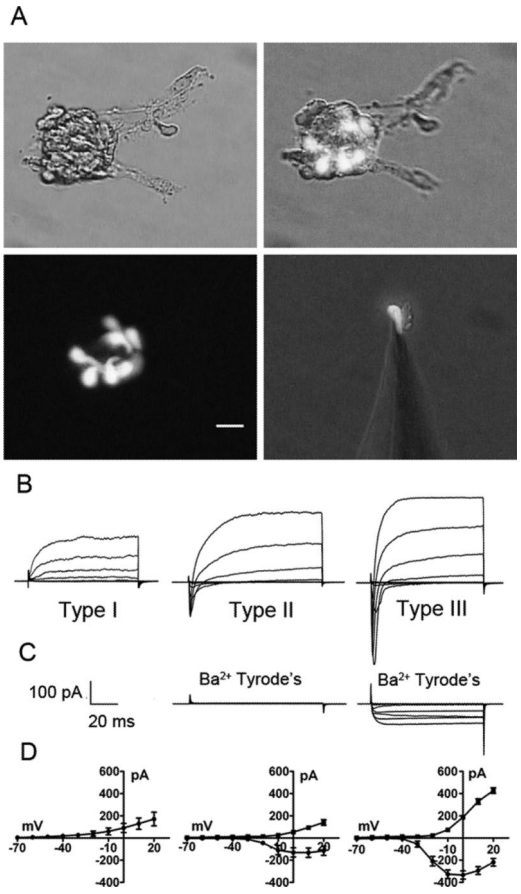

Figure 2. Optical and electrophysiological identification of taste cell type

(A) illustrates photomicrographs of circumvallate taste buds and a single isolated taste cell, isolated from a GAD67-GFP mouse, attached to a patch pipette. GFP-labeled cells are Type III taste cells. Similarly, Type II taste cells could be identified by GFP fluorescence from TrpM5-GFP mice (not shown). Calibration bar = 20 μM. (B) illustrates typical current profiles of Type I, Type II and Type III taste cells in Tyrode's. (C) Although both Type II and Type III taste cells have voltage-gated Na^+ currents in response to membrane depolarization, only Type III taste cells have voltage-gated currents in Ba^{2+} Tyrode's (with Na^+ and K^+ currents blocked) . (D) illustrates the averaged I/V curves for the voltage-gated Na^+ (circles) and K^+ (squares) currents in Type I (n=10), Type II (n=12) and Type III (n=18) in Tyrode's. Voltage was stepped in 10 mV increments from -60 mV to +20 mV from a holding potential of -70 mV.

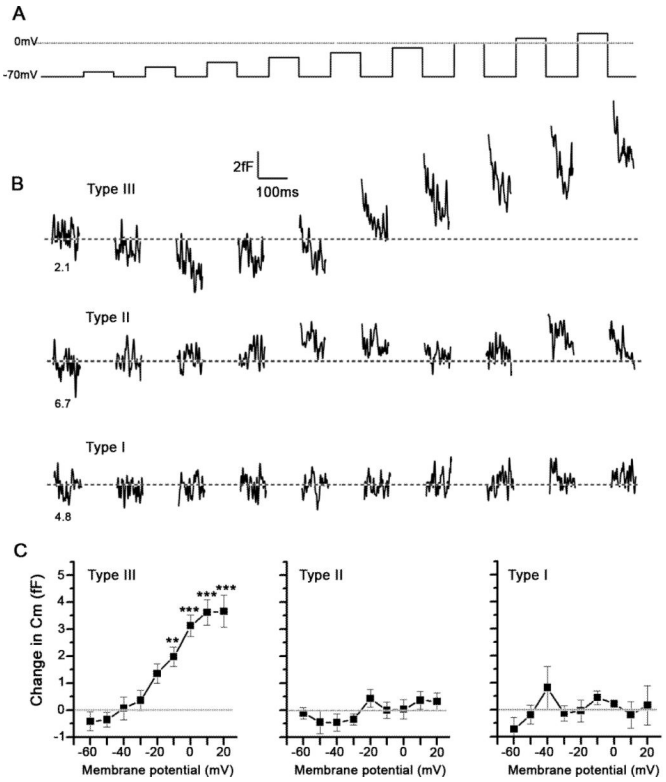

Figure 3. Type III, but not Type II and Type I taste cells exhibit voltage-induced increases in membrane capacitance (C_m)

(A) The sequence of voltage pulses, in 10 mV increments, applied to the taste cells clamped at -70 mV. (B) Representative depolarization-induced changes in C_m (100 Hz, low pass, Gaussian filter) in Type III, Type II and Type I taste cells. The numbers beneath each trace represent the resting C_m of each taste cell. (C) Average depolarization-induced changes in C_m in Type III, Type II and Type I cells, recorded in 18, 12 and 10 cells, respectively. Error bars represent SEM. The asterisks represent the significance level compared to the C_m at the first voltage step (*** P<0.001; ** P<0.01; one way ANOVA with Tukey's Multiple Comparison Test).

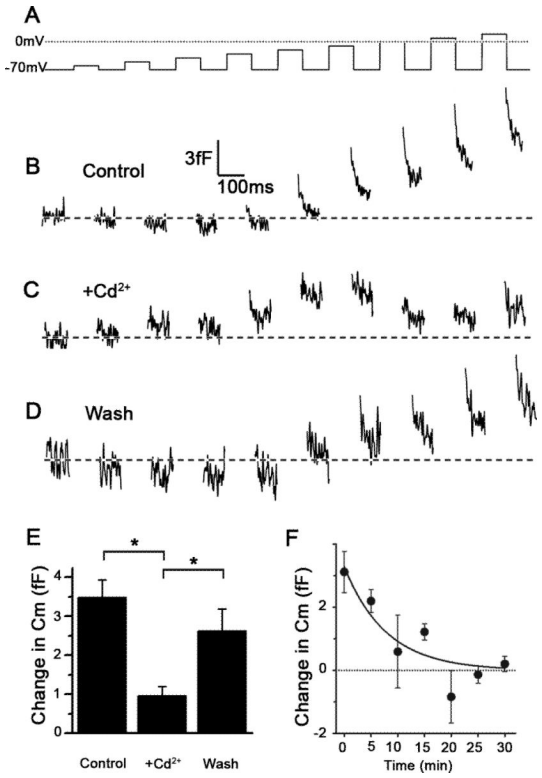

Figure 4. Cd^{2+}-mediated attenuation of voltage-induced changes in C_m in a Type III taste cell

(A) The sequence of voltage pulses applied to the taste cell clamped at -70 mV. (B) Control depolarization-induced changes in C_m, recorded before the application of Cd^{2+} Tyrode's solution. (C) Depolarization-induced changes in C_m recorded 3 minutes after the application of a Tyrode's solution containing 0.5 mM Cd^{2+}. (D) Recovery of depolarization-induced changes in C_m following 5 min wash of the cell with Tyrode's. The traces in B, C and D were low pass filtered (100Hz, Gaussian filter). (E) Average amplitude of depolarization-induced increases in C_m, determined from the last 5 voltage pulses (-20 mV to + 20 mV) on 5 cells was significantly reduced ($P<0.05$) after the application of Cd^{2+}. There was a significant (* $P<0.05$; one way ANOVA with Tukey's Multiple Comparison Test), recovery after washout of the Cd^{2+} Tyrode's. (F) Time-dependent amplitude reduction of depolarization-induced C_m in Type III taste cells (n = 6 cells). The voltage pulse protocol was applied to a single cell in 5 minute intervals. The response in C_m was averaged for the voltage pulses from -20 to +20 mV. The line represents the best fit to the equation of the form: $C_m(fF) = (3.28 \pm 0.63)e^{(0.127\pm 0.047)*time(min)}$, yielding a time-constant of the decay of around 8 minutes. Error bars represent SEM.

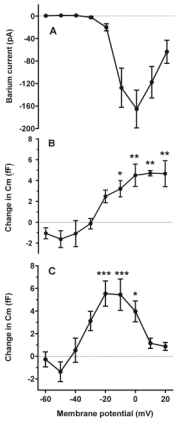

Figure 5. Relationship between the voltage pulse-induced calcium currents and the C_m change

(A) Ba2+ currents (determined in the presence of extracellular Ba^{2+}) at different membrane potentials. (B) Changes in membrane capacitance (C_m) recorded before and after the pulse were measured at the same membrane potentials in Ca^{2+}-containing Tyrode's. Cells were held at -70 mV prior to stimulating them with the voltage protocol. Each value of C_m represents the average value obtained from 10 runs (n=4 cells). (C) Changes in C_m recorded after a single voltage pulse series in a different set of taste cells (n=10 cells). Ba^{2+} currents are combined in A from both sets of cells. Error bars represent SEM. Asterisks adjacent to data points show the level of significance (*** P<0.001, ** P<0.01, *P<0.05) in comparison with the response to -60 mV; One way ANOVA with Tukey's Multiple Comparison Test).

Table 1

Maximum values of ΔC_m normalized to individual cell resting capacitance, expressed as % Max ΔC_m.

	Type III (n=18)	Type II (n=12)	Type I (n=10)
Resting Cm (pF)	2.47 ± 0.17	3.79 ± 0.50	4.06 ± 0.57
Max ΔCm at +20mV (fF)	3.67 ± 0.59	0.32 ± 0.32	0.16 ± 0.73
% Max ΔCm at +20mV	0.16 ± 0.03	0.003 ± 0.012	0.012 ± 0.03